IPSJ Transactions on Computer Vision and Applications Vol.5 119–123 (July 2013)

[DOI: 10.2197/ipsjtcva.5.119]

Express Paper

Full-dimensional Sampling and Analysis of BSSRDF

Chika Inoshita[1,a)] Seiichi Tagawa[1,b)] Md. Abdul Mannan[1,c)]
Yasuhiro Mukaigawa[1,d)] Yasushi Yagi[1,e)]

Received: March 11, 2013, Accepted: April 24, 2013, Released: July 29, 2013

Abstract: Full-dimensional (8-D) BSSRDF completely expresses the various light interactions on object surface such as reflection and subsurface scattering. However, it is difficult to sample full-dimensional BSSRDF because it requires a lot of illuminations and observations from every direction. There are many researches which approximated BSSRDF as a low-dimensional function by only considering the medium as homogeneous or assuming isotropic scattering. Therefore, in this paper, we show a novel sampling and analyzing method for full-dimensional BSSRDF in real scenes. We sample this full-dimensional BSSRDF using a polyhedral mirror system to place a lot of virtual cameras and projectors. In addition, we propose a method of decomposition of BSSRDF into isotropic and anisotropic components for scattering analysis. We show the empirical characteristics of subsurface scattering inside a real medium by analyzing sampled full-dimensional BSSRDF.

Keywords: 8-dimensional BSSRDF, subsurface scattering, BSSRDF sampling, scattering decomposition

1. Introduction

The appearance of an object is determined by interaction between its surface and the incident light. Light interaction on surface has been analyzed for understanding material perception, synthesizing realistic images, and designing industrial products. In particular, reflections on a surface have been well studied to analyze surface roughness. The reflection characteristics can be expressed by a 4-D function called bidirectional reflectance distribution function (BRDF). A variety of models which approximate the BRDF by parametric functions have been proposed in both computer graphics and computer vision fields. Alternatively, dense sampling of the BRDF becomes possible by using some optical devices [2], [6].

However, some recent research has shown that reflection is not enough to represent the real appearances of objects [4]. Most objects in our environment are not perfectly opaque, rather they have some degree of translucency. The incident light on the translucent surface scatters inside the subsurface region. That is why subsurface scattering should also be considered to analyze the surface appearance. Subsurface scattering can be completely expressed by an 8-D function called bidirectional scattering surface reflectance distribution function (BSSRDF). However, there are neither standard parametric models nor sampling methods for the 8-D BSSRDF because of its high dimensionality. Hence, researchers often conventionally approximated the BSSRDF as a low-dimensional function by considering only the medium as homogeneous [1] or assuming isotropic scattering based on diffusion theory [3].

In this paper, we show a novel sampling and analyzing method for full-dimensional BSSRDF in real scenes. We sample this full-dimensional BSSRDF using a polyhedral mirror system to place a lot of virtual cameras and projectors. We analyze the sampled BSSRDF by visualizing some 4-D slices. In addition, we propose a method of decomposition of BSSRDF into isotropic and anisotropic components for scattering analysis.

Contribution

- This research is the first trial to sample and analyze full-dimensional (8-D) BSSRDF to treat inhomogeneous translucent material such as marble.
- Traditional models assume that the BSSRDF consists of single and multiple scatterings. Instead, we decompose the BSSRDF into isotropic and anisotropic components to analyze directional distribution. This decomposition becomes possible because 8-D includes all angular information.

2. Definition of 8-D BSSRDF

When a translucent object is illuminated, some parts of the incident light penetrate inside the subsurface. After scattering by material particles, some parts of light get back to the first medium through different points on the object surface as illustrated in **Fig. 1**.

This subsurface scattering depends on the incident point $\boldsymbol{x}_i = (x_i, y_i)$ and outgoing point $\boldsymbol{x}_o = (x_o, y_o)$ as well as incident direction $\boldsymbol{\omega}_i = (\theta_i, \phi_i)$ and outgoing direction $\boldsymbol{\omega}_o = (\theta_o, \phi_o)$. Hence, the

[1] The Institute of Scientific and Industrial Research, Osaka University, Ibaraki, Osaka 567–0047, Japan
[a)] inoshita@am.sanken.osaka-u.ac.jp
[b)] tagawa@am.sanken.osaka-u.ac.jp
[c)] mannan@am.sanken.osaka-u.ac.jp
[d)] mukaigaw@am.sanken.osaka-u.ac.jp
[e)] yagi@am.sanken.osaka-u.ac.jp

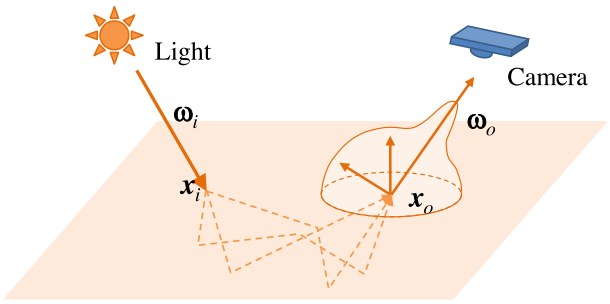

Fig. 1 Subsurface scattering. Incident light penetrates surface, and repeats scattering inside subsurface region. Finally, the light emits from different surface points.

subsurface scattering can be expressed by the BSSRDF as

$$f(\boldsymbol{x}_i, \boldsymbol{\omega}_i, \boldsymbol{x}_o, \boldsymbol{\omega}_o). \quad (1)$$

The BSSRDF is an eight dimensional function defined by four positional parameters and four angular parameters.

3. Analysis of Full-dimensional BSSRDF

If we assume a homogeneous material or diffusion theory, the dimension of the BSSRDF can be reduced [3]. However, it is difficult to represent real scattering accurately based on only approximated low-dimensional functions. In this section, we show how to sample and analyze full-dimensional BSSRDF.

3.1 Sampling Using Polyhedral Mirror System

If we want to sample BSSRDF, we need to surround the target object with a lot of cameras and projectors. Obviously, such large numbers of devices are impractical. Therefore, mirror systems [5], [9] are often used to produce many virtual cameras and projectors. These mirror systems are designed for special imaging methods such as shallow DOF imaging and confocal imaging. In our previous research [9] we have already developed the *Turtleback Reflector* as shown in **Fig. 2** (a). The reflector was designed to distribute many virtual cameras and projectors on a hemisphere with uniform density and constant distance. Combining the reflector with a camera and a projector, we can observe and illuminate from a wide area on a hemisphere. We reuse this system for sampling full-dimensional BSSRDF.

The sampling densities of incident position $\boldsymbol{x}_i$ and outgoing position $\boldsymbol{x}_o$ are 20 by 20 and 100 by 100, respectively. The number of sampling direction of $\boldsymbol{\omega}_i$ and $\boldsymbol{\omega}_o$ is 48. **Figure 3** shows the position of the virtual cameras and projectors. In total, 19,200 (48 incident directions × 20 by 20 resolution) images are captured for BSSRDF sampling. If the shutter speed is set to 100 ms, the total sampling time becomes 32 minutes. Although the sampling is sparse, full-dimensional (8-D) BSSRDF can be obtained using our optical device.

We have sampled BSSRDFs of three different materials; (a) epoxy resin, (b) rubber eraser, and (c) marble as shown in **Fig. 4**. These materials have different properties of translucency. The epoxy resin is optically thin, while the rubber eraser is optically dense. The marble is a typical inhomogeneous material. Square regions indicated by red broken lines show the sampling areas. **Figure 5** shows captured images enhanced by gamma correction ($\gamma = 2.0$). The left column of Fig. 5 shows captured images by

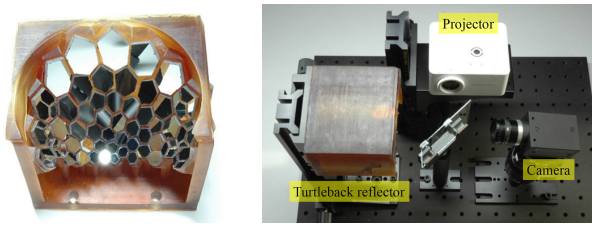

(a) *Turtleback Reflector* (b) System overview

Fig. 2 *Turtleback Reflector* [9]. The combination of the reflector with a camera and a projector, many virtual cameras and projectors can be distributed on a hemisphere.

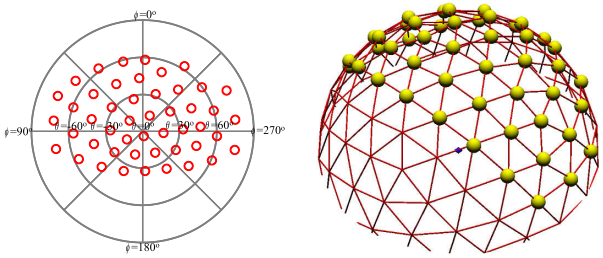

Fig. 3 Sampling positions on a hemisphere. Left: virtual cameras and projectors are placed uniformly. Right: the sampling positions correspond to the vertexes of the geodesic dome.

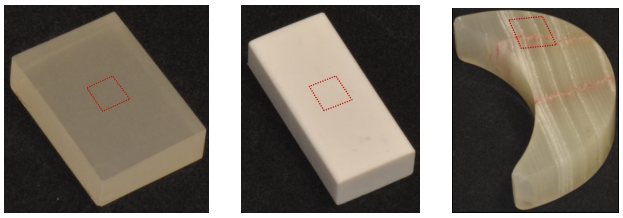

(a) epoxy resin (b) rubber eraser (c) marble

Fig. 4 Target translucent materials. The epoxy resin is optically thin, while the rubber eraser is optically dense. The marble is a typical inhomogeneous material. Square regions indicated by red broken lines show the sampling areas.

different virtual cameras under the same incident light. These are 4-D $(\boldsymbol{x}_o, \boldsymbol{\omega}_o)$ slices of the sampled BSSRDFs under fixed illumination $\boldsymbol{x}_i = (0, 0)$ and $\boldsymbol{\omega}_i = (2.2°, 154.3°)$. Each small block shows brightness at each $\boldsymbol{x}_o$ from the particular outgoing direction $\boldsymbol{\omega}_o$. The right column of Fig. 5 shows captured images by the same virtual camera under different incident lights. These are 4-D $(\boldsymbol{x}_o, \boldsymbol{\omega}_i)$ slices sampled from the fixed incident point $\boldsymbol{x}_i = (0, 0)$ and outgoing direction $\boldsymbol{\omega}_o = (2.2°, 154.3°)$. Since color bleeding is occurred in captured images due to color filter pattern of the projector, we analyze scattering intensities in grayscale.

We can see that anisotropic single scatterings are observed in the epoxy resin, while isotropic multiple scattering is dominant in the rubber eraser. Since the marble has an inhomogeneous structure including both optically thin and dense parts, spatially-varying scatterings are observed.

3.2 Analysis of Sampled BSSRDF

In this section, we analyze the sampled BSSRDFs. It is difficult to directly show the 8-D information. Hence, we visualize several low-dimensional slices of the sampled BSSRDFs.

Figure 6 shows 4-D slices $(x_o, y_o, \theta_o, \phi_o)$ of the BSSRDF at several (x_i, y_i) as 6-D slices $(x_i, y_i, x_o, y_o, \theta_o, \phi_o)$ of the BSSRDF. Direction of illumination is fixed at $(\theta_i, \phi_i) = (44.9°, 74.8°)$. We

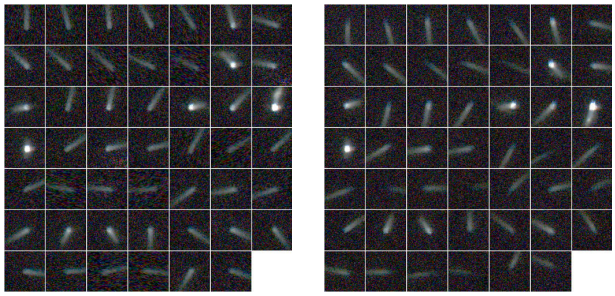

(a) epoxy resin

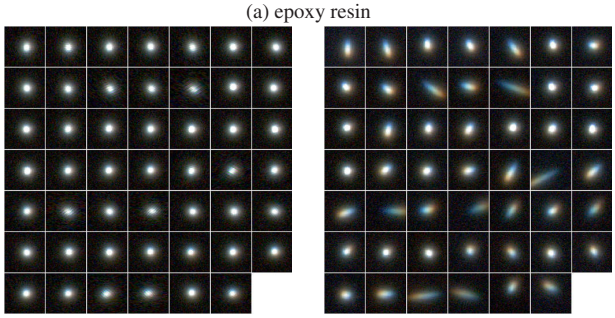

(b) rubber eraser

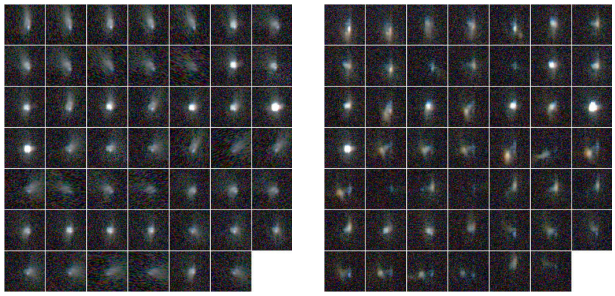

(c) marble

Fig. 5 Some examples of captured images by virtual cameras. The left column shows captured images by different virtual cameras under the same incident light. The right column shows captured images by the same virtual camera under different incident lights. These images are enhanced by gamma correction ($\gamma = 2.0$).

plot the value of BSSRDF at (x_o, y_o) from -40 to 40 at 10 intervals for all viewing directions in log scale pseudo color. **Figure 7** shows illuminated positions (x_i, y_i) on each material. The upper and lower rows in Fig. 6 show 4-D slices of BSSRDF given by illumination at the red and blue points in Fig. 7, respectively. Figure 6 (a) shows slices of BSSRDF of epoxy resin in which strong single scattering occurs. The spatial distribution has peak values along the azimuth angle of the direction of illumination because single scattering depends on refractive direction of incident light. Additionally, slices of BSSRDFs are quite similar despite different incident positions because epoxy resin is a homogeneous media. Figure 6 (b) shows that the spatial distribution of a rubber eraser has no specific propagation direction due to multiple scattering. BSSRDF slices of a rubber eraser given by different incident points are also similar due to homogeneousness. Figure 6 (c) shows the visualized BSSRDF of marble. Because marble is optically thin, light propagates in a particular spatial region as same as epoxy resin. However, slices of BSSRDFs given by different incident positions are not same due to its inhomogeneous structure. Since 8-D BSSRDF includes spatial information such as incident/outgoing position, we can analyze spatial structure based on similarity of BSSRDF slice.

Figure 8 shows 6-D slices $(\theta_i, \phi_i, x_o, y_o, \theta_o, \phi_o)$ of the BSSRDF. Red distribution is given by direction of illumination $(\theta_i, \phi_i) = (44.3°, 127.2°)$, and blue distribution is given by $(\theta_i, \phi_i) = (43.7°, 233.7°)$. Directions of illumination are almost symmetric. Optically thin materials such as epoxy resin and marble changes the shape of the distribution according to the direction of illumination and distributions at each point are anisotropic. Light distributions of optically dense rubber eraser do not change along to incident angles. Additionally, distributions at each incident point are isotropic. For any material, angular distributions along to direction of illumination also represents optical characteristics of material.

Finally, we confirm the accuracy of the dipole approximation model [3] using sampled BSSRDF of a rubber eraser. In the field of computer graphics, optically dense translucent materials are often synthesized based on a dipole model. The BSSRDF based on dipole approximation is represented as

$$f(\boldsymbol{x}_i, \boldsymbol{\omega}_i, \boldsymbol{x}_o, \boldsymbol{\omega}_o) = \frac{1}{\pi} F_t^o(\eta, \boldsymbol{\omega}_o) R(\boldsymbol{x}_i, \boldsymbol{x}_o) F_t^i(\eta, \boldsymbol{\omega}_i), \tag{2}$$

where $R(\boldsymbol{x}_i, \boldsymbol{x}_o)$ represents scattering term of dipole model parameterized by scattering coefficient σ_s', absorption coefficient σ_t, and refractive index η. $F_t(\eta, \boldsymbol{\omega})$ represents Fresnel transmission function. From Eq. (2), BSSRDF with arbitrary $\boldsymbol{\omega}_i$ and $\boldsymbol{\omega}_o$ corresponds to BSSRDF with interchanged $\boldsymbol{\omega}_i$ and $\boldsymbol{\omega}_o$. **Figure 9** shows the result of dipole model fitting. Sampled BSSRDFs are plotted by dot. Blue dots show sampled BSSRDF with $(\theta_i, \phi_i) = (2.2°, 154.3°)$ and $(\theta_i, \phi_i) = (43.7°, 233.7°)$ and orange dots show BSSRDF with interchanged illumination and observation angles. Fitting results are shown by solid lines. We normalize BSSRDF as $f(\boldsymbol{x}_i, \boldsymbol{\omega}_i, \boldsymbol{x}_o, \boldsymbol{\omega}_o) = 1$ at $|\boldsymbol{x}_i - \boldsymbol{x}_o| = 0$ and set refractive index $\eta = 1.3$. As shown in Fig. 9, sampled BSSRDFs are quite similar. This observation satisfies the model described as Eq. (2). Additionally, BSSRDFs are approximated in low error. From this result, we confirm that the appearance of rubber eraser can be approximated based on a dipole model.

If the BSSRDF is represented by an approximated low-dimensional function, it is difficult to analyze both spatial and angular distributions simultaneously. Our detailed analysis is realized by full-dimensional BSSRDF sampling.

3.3 Decomposition of Isotropic and Anisotropic Components

To analyze light interaction on the object surface, it is important to decompose observed phenomenon into basic optical components. Since traditional photometric methods have assumed only diffuse reflection, surface reflection is often decomposed into diffuse and specular reflection components to remove faulty causes [7]. Nishino et al. [8] focused on the angular dependency of surface reflection, and decomposed angular dependent specular reflection and angular independent diffuse reflection. Inspired by their method, we decompose observed BSSRDF based on angular dependency.

In the previous section, we have shown various directional dependencies of the scattered lights. That is, the BSSRDF also can be decomposed into the angular independent isotropic component and angular dependent anisotropic component as illustrated in **Fig. 10**. The isotropic component does not depend on the view-

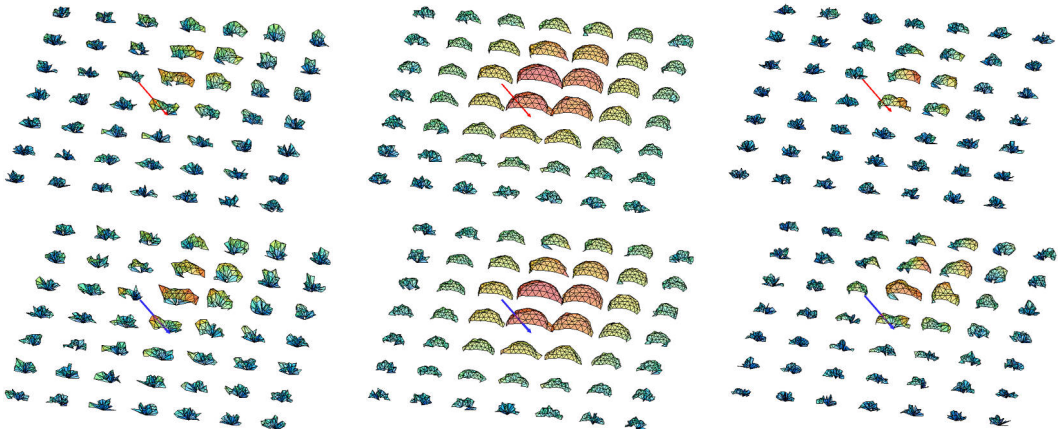

(a) epoxy resin (b) rubber eraser (c) marble

Fig. 6 Visualized BSSRDF. Direction of illumination is fixed at $(\theta_i, \phi_i) = (44.9°, 74.8°)$. The top row in (a)-(c) shows visualizations of BSSRDF from illumination at red point in Fig. 7. The bottom row in (a)-(c) shows visualizations of BSSRDF from fixed illumination at blue point in Fig. 7. The red arrow represents the direction of illumination.

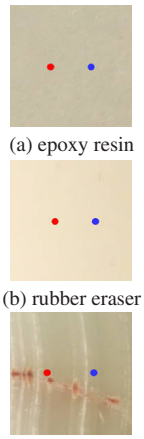

(a) epoxy resin (b) rubber eraser (c) marble

Fig. 7 Illuminated positions for visualization on each material.

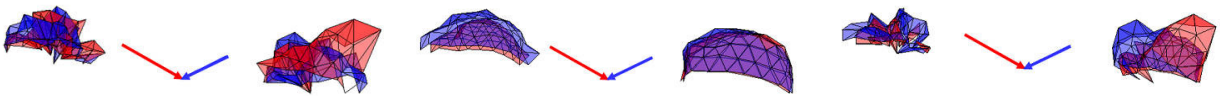

(a) epoxy resin (b) rubber eraser (c) marble

Fig. 8 Close up of visualized BSSRDF. We show angular distribution at $(x_o, y_o) = (-10, 0), (10, 0)$. The red arrow represents the direction of illumination $(\theta_i, \phi_i) = (44.3°, 127.2°)$ and the blue arrow also represents the direction of illumination $(\theta_i, \phi_i) = (43.7°, 233.7°)$. Blue and red distributions represent the visualized angular distribution given by each illumination.

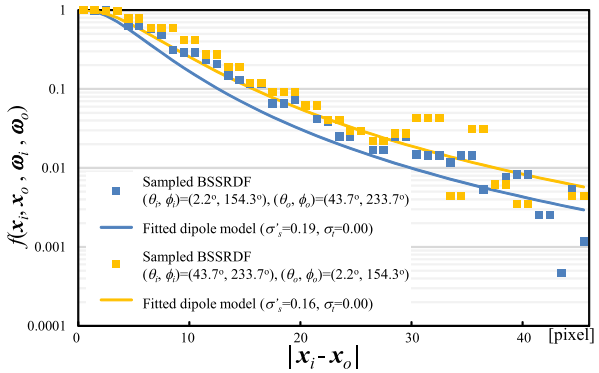

Fig. 9 Result of dipole model fitting. Dots show sampled BSSRDF at each ω_i, ω_o. Solid lines show fitted dipole model.

ing direction, while the anisotropic component varies according to the viewing direction. We formulate the decomposition by

$$f(\boldsymbol{x}_i, \boldsymbol{\omega}_i, \boldsymbol{x}_o, \boldsymbol{\omega}_o) = f_i(\boldsymbol{x}_i, \boldsymbol{\omega}_i, \boldsymbol{x}_o) + f_a(\boldsymbol{x}_i, \boldsymbol{\omega}_i, \boldsymbol{x}_o, \boldsymbol{\omega}_o), \tag{3}$$

where the function f_i represents the isotropic component and the function f_a represents the anisotropic component. It is noted that the argument $\boldsymbol{\omega}_o$ is not included in the function f_i because of independency on viewing directions.

These two components are decomposed based on the constancy of the angular distribution. To implement this idea, we refer to a separation method proposed by Nishino et al. [8]. In that work they simply extracted view-independent components by taking the minimal pixel value at each surface point as constant component over image sequences. We also apply this idea to decompose sampled BSSRDFs. The isotropic component is separated by finding the minimal value along viewing directions at each surface point by

$$f_i(\boldsymbol{x}_i, \boldsymbol{\omega}_i, \boldsymbol{x}_o) = \min_{\boldsymbol{\omega}_o \in \boldsymbol{\Omega}} f(\boldsymbol{x}_i, \boldsymbol{\omega}_i, \boldsymbol{x}_o, \boldsymbol{\omega}_o), \tag{4}$$

where $\boldsymbol{\Omega}$ denotes hemispherical directions. Then, the anisotropic component is computed as residual by

$$f_a(\boldsymbol{x}_i, \boldsymbol{\omega}_i, \boldsymbol{x}_o, \boldsymbol{\omega}_o) = f(\boldsymbol{x}_i, \boldsymbol{\omega}_i, \boldsymbol{x}_o, \boldsymbol{\omega}_o) - f_i(\boldsymbol{x}_i, \boldsymbol{\omega}_i, \boldsymbol{x}_o). \tag{5}$$

Figure 11 shows the decomposition results of sampled BSSRDFs of epoxy resin, rubber eraser and marble. The left column shows the sum of sampled BSSRDFs for all observation directions E_{both}, the center column shows the sum of decomposed anisotropic BSSRDF for all observation directions E_a and the right column shows the scaled decomposed isotropic BSSRDFs E_i as

$$E_{both} = \sum_{\boldsymbol{\omega}_o} f(\boldsymbol{x}_i, \boldsymbol{\omega}_i, \boldsymbol{x}_o, \boldsymbol{\omega}_o), \tag{6}$$

$$E_a = \sum_{\boldsymbol{\omega}_o} f_a(\boldsymbol{x}_i, \boldsymbol{\omega}_i, \boldsymbol{x}_o, \boldsymbol{\omega}_o), \tag{7}$$

$$E_i = s f_i(\boldsymbol{x}_i, \boldsymbol{\omega}_i, \boldsymbol{x}_o). \tag{8}$$

Since epoxy resin shows high directional scattering, most of the light is categorized in the anisotropic component. On the other hand, strong multiple scattering in rubber eraser is categorized in the isotropic component. Illuminated light gradually loses its directivity as the light scatters; low-bounce scattering keeps the directivity of illumination, while high-order scattering loses directivity. Hence, we often see anisotropic scattering in optically thin media and isotropic scattering in optically dense media. This result shows that we can decompose the scattering component

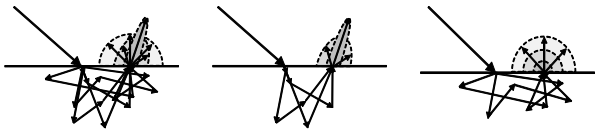

(a) Both components (b) Anisotropic component (c) Isotropic component

Fig. 10 Concept of decomposition. We decompose sampled BSSRDFs into isotropic and anisotropic components based on the directional dependency.

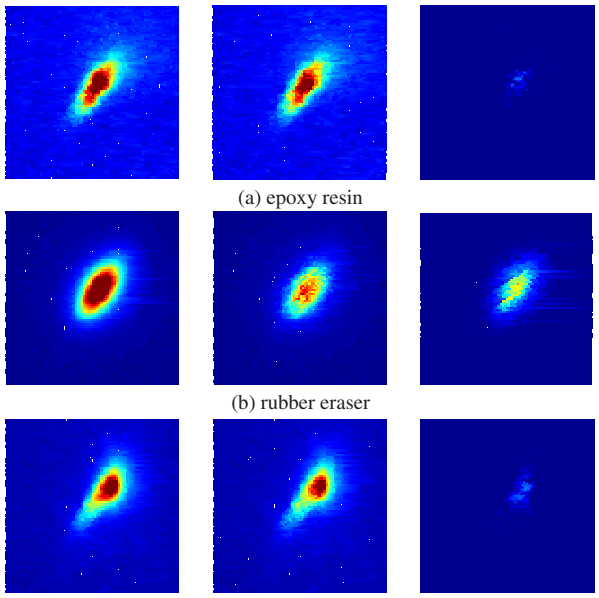

(a) epoxy resin (b) rubber eraser (c) marble

Fig. 11 Decomposition results for three materials. The left column shows both components, the center column shows the decomposed anisotropic component and the right column shows the decomposed isotropic component. Each image shows the total energies of emitted light at each surface point.

into low-bounce and high-order scatterings based on the angular dependency, and the angular dependency can be a clue to analyze optical density. Marble has a low isotropic component because its inhomogeneous structure generates angular varying distribution. From this result, the spatial structure of an object also affects angular dependency of scattered light. Even though an object is optically dense, anisotropic scattering dominates the observed scattering in inhomogeneous structure.

From these decomposed results, we confirmed that the sampled BSSRDFs can be decomposed into isotropic and anisotropic components by angular analysis. In addition, we can analyze optical characteristics from decomposed light.

4. Discussion and Summary

In this paper, we have presented a method to sample and analyze full-dimensional BSSRDFs. For sampling, we used the *Turtleback Reflector* which is a polyhedral mirror system to illuminate and observe the object surface from various directions. For analysis, we visualized spatial and angular distributions by slicing BSSRDFs. In addition, we decomposed BSSRDF into isotropic and anisotropic components. From this analysis, it is revealed that the ratio of two components strongly depends on the optical density and homogeneousness of the medium. In the future, we will make a BSSRDF database of a variety of materials and formulate parametric models based on the physical analysis.

Acknowledgments This research is granted by the Japan Society for the Promotion of Science (JSPS) through the "Funding Program for Next Generation World-Leading Researchers (NEXT Program)," initiated by the Council for Science and Technology Policy (CSTP).

References

[1] Donner, C., Lawrence, J., Ramamoorthi, R., Hachisuka, T., Jensen, H.W. and Nayar, S.: An Empirical BSSRDF Model, *Proc. SIGGRAPH2009*, pp.30:1–30:10 (2009).
[2] Ghosh, A., Achutha, S., Heidrich, W. and O'Toole, M.: BRDF Acquisition with Basis Illumination, *Proc. ICCV2007*, pp.1–8 (2007).
[3] Jensen, H.W., Marschner, S.R., Levoy, M. and Hanrahan, P.: A Practical Model for Subsurface Light Transport, *Proc. SIGGRAPH2001*, pp.511–518 (2001).
[4] Kurachi, N.: *The Magic of Computer Graphics*, CRC Press (2011).
[5] Levoy, M., Chen, B., Vaish, V., Horowitz, M., McDowall, I. and Bolas, M.: Synthetic Aperture Confocal Imaging, *Proc. SIGGRAPH2004*, pp.825–834 (2004).
[6] Mukaigawa, Y., Sumino, K. and Yagi, Y.: Rapid BRDF Measurement using an Ellipsoidal Mirror and a Projector, *IPSJ Trans. Computer Vision and Applications*, Vol.1, pp.21–32 (2009).
[7] Nayar, S.K., Fang, X.-S. and Boult, T.: Separation of Reflection Components Using Color and Polarization, *International Journal of Computer Vision*, Vol.21, pp.163–186 (1997).
[8] Nishino, K., Zhang, Z. and Ikeuchi, K.: Determining Reflectance Parameters and Illumination Distribution from a Sparse Set of Images for View-dependent Image Synthesis, *Proc. ICCV2001*, pp.599–606 (2001).
[9] Tagawa, S., Mukaigawa, Y., Kim, J., Raskar, R., Matsushita, Y. and Yagi, Y.: Hemispherical Confocal Imaging, *IPSJ Trans. Computer Vision and Applications*, Vol.3, pp.222–235 (2011).

(Communicated by *Takayuki Okatani*)